Soft Matter

PAPER

View Article Online
View Journal | View Issue

Cite this: *Soft Matter*, 2014, **10**, 4833

Self-assembly of an azobenzene-containing polymer prepared by a multi-component reaction: supramolecular nanospheres with photo-induced deformation properties†

Shuai Wang, Ning Zhang, Xiaopeng Ge, Yingbo Wan, Xiaohong Li, Li Yan, Yijun Xia and Bo Song*

Received 27th March 2014
Accepted 28th April 2014

DOI: 10.1039/c4sm00675e

www.rsc.org/softmatter

In this article, we have synthesized a polymer containing regulated azobenzene groups by one-pot multi-component polymerization (MCP) based on Passerini reaction, and investigated its self-assembly behavior and photo-induced deformation properties. We found that this molecule can form spherical structures with sizes ranging from hundreds of nanometers to several micrometers when dissolved in THF. NMR and FTIR studies indicate that there are associated hydrogen bonds among the molecules in the aggregates, which are responsible for the formation of the nanospheres. By controlling the stirring rate as the THF suspension is dropped into water, the nanospheres can be sorted according to their size. In this way, we have obtained nanospheres with relatively uniform diameter. When irradiated by UV light in the aqueous medium, the nanospheres tend to aggregate into large clusters, while in dry state they are ready to merge into island-like structures, showing a good photo-induced deformation property.

I Introduction

Polymers with photo-induced deformation properties are a new type of advanced functional materials.[1–12] Upon the external light stimuli, the polymers containing photochromic dyes, such as azobenzene,[13–29] spiropyran[30,31] or malachite green,[32] carry out a macroscopic movement (contraction or extension). This unique property can be expanded to practical applications like surface relief gratings,[33–39] artificial muscles,[29,40] photo-driven actuators[13,29,41–44] and oscillators.[45,46] At the microscopic scale, this concept can also be employed to manipulate the morphologies of the basic constructive elements, in applications of deformable colloidal spheres,[47–52] optical data storage,[49] and controlled release.[52–56] In fabricating such kinds of microscopic structures, the anisotropic nature (mostly the amphiphilic characters) of block copolymers is widely designed and utilized.[21,57–60] Preparation of the functional copolymers is normally achieved through two-step polymerizations, and it is sometimes followed by grafting of the photochromic groups. Herein, we would like to seek a more efficient way to fabricate micro-structures with photo-induced deformation properties. For fulfilling this purpose: (1) we attempt to design and synthesize a polymer with regulated functional groups, and use it as building blocks for self-assembly; (2) supramolecular interactions would be designed for the driving force for the assembly; and (3) a suitable and facile polymerization method would be optionally pursued.

Passerini reaction has advantages such as mild reaction conditions, atom economy, and tolerance to many functional groups.[61–64] The recently developed multi-component polymerization (MCP) based on Passerini reaction has been demonstrated to be a feasible, easy, and efficient method to prepare functional polymers.[65–67] In addition, the polymers prepared by this method can be endowed with a sequence-regulated backbone, which would be a fascinating feature for self-assembly *via* supramolecular interactions.

In this article, we have prepared a polymer bearing regulated azobenzene functional groups by a MCP method. Similar to traditional amphiphilic copolymers, this polymer can also self-assemble into spherical nanostructures. Atomic force microscopy (AFM) and transmission electron microscopy (TEM) investigations indicate that these nanospheres show photo-induced deformation properties both in a liquid and dry state. We hope this line of research can supply a new clue for constructing photo-stimulated functional materials.

Jiangsu Key Laboratory of Advanced Functional Polymer Design and Application, The Key Lab of Health Chemistry and Molecular Diagnosis of Suzhou, College of Chemistry, Chemical Engineering and Materials Science, Soochow University, Suzhou 215123, P. R. China. E-mail: songbo@suda.edu.cn; Tel: +86 (512) 65882507

† Electronic supplementary information (ESI) available: ^{1}H NMR spectra, concentration dependent tubidity, DLS data, gCOSY spectra, gHSQC spectra, gHMBC spectra, TEM & AFM images, and FTIR spectra. See DOI: 10.1039/c4sm00675e

II Experimental

Materials

Hexane-1,6-diamine, ethyl formate, dichloromethane, triethylamine, K_2CO_3, $NaIO_4$, silica gel, $NaNO_2$, NaOH, phenol, THF, and ethyl ether were purchased from Sinopharm Chemical Reagent Co., Ltd. and used as received. *trans*-Cyclohexane-1,2-diol was purchased from Alfa Aesar China (Tianjin) Co., Ltd. Phosphoryl trichloride was bought from Gracia Chengdu Chemical Company. 4-(4-Amino phenyl)butanoic acid was purchased from Shanghai Boyle Chemical Co., Ltd. Ammonium sulfamate was purchased from Tokyo Chemical Industry Co., Ltd. $CDCl_3$, CD_3OD and DMSO-d_6 were bought from J & K Technology Co., Ltd. Deionized and distilled water was used in all the experiments.

Synthesis of 1,6-diisocyanohexane (A in Scheme 1)

A solution of hexane-1,6-diamine (11.6 g, 0.1 mol) in 100 mL ethyl formate was refluxed for 5 h. Then, the solvent was removed by vacuum evaporation. The crude product was used in the next step without further purification. About 0.1 mol of formamide was suspended in 200 mL anhydrous dichloromethane, and then 51 g (0.5 mol) triethylamine was added. The mixture was cooled to 0 °C, and 32 g (0.2 mol) of phosphoryl trichloride was added dropwise such that the reaction temperature was maintained below 0 °C. After being stirred for 2 h, the reactant was poured into a 500 mL beaker with 200 mL ice–water mixture containing 100 g of K_2CO_3. During the above operation, the temperature was maintained below 25 °C. The resulting emulsion was stirred for 1 h at room temperature. The organic layer was removed, and the aqueous layer was extracted with dichloromethane. Then, the combined organic layer was collected and dried with anhydrous K_2CO_3. After evaporation of the solvent, the residue was purified by aluminium oxide column chromatography (CH_2Cl_2–hexane, 1 : 1) to give a pale brown liquid (9.4 g). Yield: 69%. ^{1}H-NMR (300 MHz, $CDCl_3$, 25 °C, TMS), δ (ppm): 3.40 (m, 4H, CH_2NC), 1.70 (m, 4H, CH_2CH_2NC), 1.48 (m, 4H, $CH_2CH_2CH_2$NC).

Synthesis of adipaldehyde (B in Scheme 1)

First, 60 mL aqueous solution of $NaIO_4$ (1.1 mol L^{-1}) was heated to 70 °C, and then added to the aqueous suspension of silica gel (50 g) with stirring. Afterwards, a solution of *trans*-cyclohexane-1,2-diol (5.8 g, 50 mmol) in CH_2Cl_2 (250 mL) was added dropwise into the suspension. Then, the mixture was cooled to room temperature and continuously stirred for 24 h. After the silica gel was filtered out, the solvent was removed by vacuum evaporation, giving a colorless oil (5.2 g). Yield: 89%. ^{1}H-NMR (300 MHz, $CDCl_3$, 25 °C, TMS), δ (ppm): 9.40 (t, J = 1.4 Hz, 2H, *CH*O), 2.15 (m, 4H, CH_2CHO), 1.31 (m, 4H, CH_2CH_2CHO).

Synthesis of 4-(4-((4-hydroxyphenyl)diazenyl)phenyl)butanoic acid (C in Scheme 1)

In a 1000 mL flask, 200 mL of 0.1 mol L^{-1} HCl was added and cooled to 5 °C by ice bath, and then with stirring 1.25 g (7.0 mmol) of 4-(4-amino phenyl)butanoic acid and 0.48 g (7.0 mmol) of $NaNO_2$ were added. After the solid had dissolved, 0.80 g (7.0 mmol) of ammonium sulfamate was added, followed by immediate addition of a solution of 320 mL of 0.1 mol L^{-1} NaOH containing phenol (0.72 g, 7.8 mmol). Then, the solution was adjusted to pH = 3 by adding 2 mol L^{-1} HCl, and the precipitate was filtered out and washed with water. The solid was then dried under vacuum and purified by silica gel chromatography. The resultant product is a brown powder (1.2 g). Yield: 61%. ^{1}H-NMR (300 MHz, CD_3OD, 25 °C, TMS), δ (ppm): 7.82 (d, J = 8.7 Hz, 2H, *m*-PhOH), 7.79 (d, J = 7.5 Hz, 2H, *o*-azophenyl), 7.37 (d, J = 8.4 Hz, 2H, *m*-azophenyl), 6.93 (d, J = 8.7 Hz, 2H, *o*-PhOH), 2.74 (t, J = 7.5 Hz, 2H, CH_2COOH), 2.34 (t, J = 7.2 Hz, 2H, $CH_2CH_2CH_2$COOH), 2.01 (m, 2H, CH_2CH_2COOH).

MCP based on Passerini reaction

In an eggplant-shaped flask, 0.57 g (2 mmol) 4-(4-((4-hydroxyphenyl)diazenyl)phenyl)butanoic acid was added along with 2 mL THF. Then, 0.11 g (1 mmol) adipaldehyde and 0.14 g (1 mmol) 1,6-diisocyanohexane were added. The mixture was stirred under nitrogen atmosphere at 45 °C for 48 h. Then, the solution was diluted with THF, and the product was precipitated in cold ethyl ether and separated by filtration. The precipitation and filtration was repeated two more times. Then, the obtained polymer was dried in vacuum and stored in a desiccator. The chemical shifts of the resultant product are defined in ESI (Fig. S1†).

Instruments

^{1}H NMR spectra of the monomers were obtained on an NMR system 300 (manufactured by Varian) operating at a frequency of 300 MHz. ^{1}H NMR spectra of the polymer were collected at 25 °C on an Agilent Direct-Drive II 600 MHz spectrometer.

Liquid chromatography-mass spectroscopy analyses were performed on an Aglient 6120 Quadrupole system with ESI resource produced by Agilent Technologies (USA).

The molecular weight and molecular weight distribution of the resultant polymer were determined by gel permeation chromatography (GPC) using a Waters 1515 gel permeation chromatograph. During the measurement, DMF was selected as the eluent at a flow rate of 1.0 mL min^{-1}, and the operating temperature was controlled at 50 °C. GPC samples were injected using a Waters 717 plus auto sampler and calibrated with poly(methyl methacrylate) standards purchased from Waters.

Scanning electron microscopy (SEM) images were recorded on a Hitachi S-4800 (Japan). TEM characterization was performed using a Hitachi HT7700 (Japan) operating at 120 kV. The samples were casted on carbon-coated copper grids and measured without staining. AFM images were recorded on a Multimode 8 microscope (Bruker, Santa Barbara, CA, USA). Peak force quantitative nano-mechanical scan mode with Scan Asyst-Air probe (nominal spring constants 0.4 N m^{-1}, frequency 70 kHz, from Bruker) was adopted during the measurement. Dynamic light scattering (DLS) was measured at ambient conditions using a Zetasizer Nano-ZS (Malvern Instruments,

UK) equipped with a 633 nm He–Ne laser and back-scattering detector.

Fourier transform infrared (FTIR) spectra were obtained using a Nicolet 6700 produced by Thermo Scientific (USA). The sample was prepared by casting the THF suspension on calcium fluoride substrates, and then drying in vacuum.

The UV-vis spectra of the samples were measured over different irradiation time intervals using a UV-Vis spectrometer Cary 60 produced by Agilent Technologies (USA). The UV irradiation on the samples was carried out with a fiber lamp SP-9 equipped with a high-intensity UV source UXM-Q256BY produced by USHIO (Japan).

III Results and discussion

As shown in Scheme 1, an azobenzene-containing polymer, denoted as MCP-azo-OH, was synthesized by MCP based on Passerini reaction (see the details in the Experimental section). The molecular weight determined by GPC is 6.5 kDa, indicating that the resulting compound contains approximately 7 azobenzene repeat units.

To our surprise, MCP-azo-OH shows a very good self-assembly property. Even when dissolved in THF (which is a selective solvent indicated by scattering changes at different concentrations, as shown in Fig. S2 in the ESI†), the solution shows a strong Tyndall effect, suggesting that the molecules have self-assembled into some aggregates. The morphology of the aggregates was imaged by SEM, TEM, and AFM (the specimens are prepared from solution with a polymer concentration of 0.5 mg mL^{-1}). As shown in Fig. 1, all the images indicate that MCP-azo-OH forms spherical nanoparticles with sizes ranging from hundreds of nanometers to several micrometers, which is consistent with the DLS data (Fig. S3 in the ESI†). The dark dots in the TEM image (Fig. 1b) show a uniform contrast, which demonstrates that the nanospheres are not hollow inside. The spherical feature can also be reflected from the comparative height and the half-height width of the nanospheres shown in the section analysis of the AFM image (Fig. 1d).

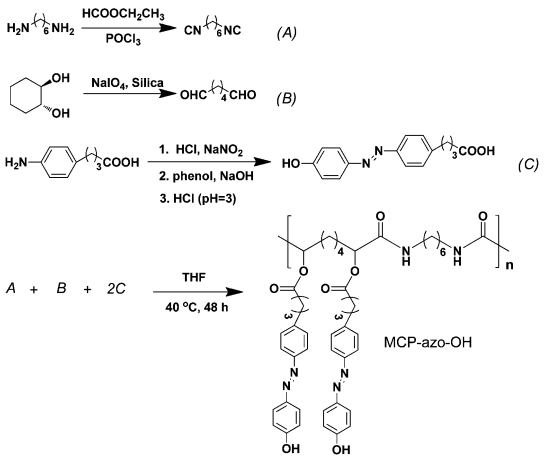

Scheme 1 Synthetic route of MCP-azo-OH.

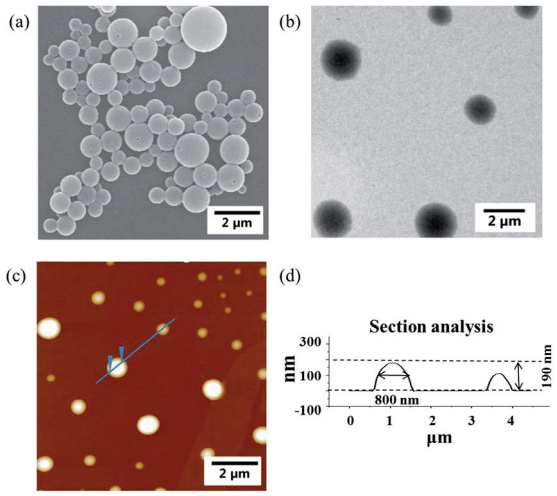

Fig. 1 (a) SEM image, (b) TEM image, and (c) AFM image of the nanospheres obtained from the THF suspension, which was prepared by stirring the solution (0.5 mg mL^{-1}) of MCP-azo-OH at room temperature for at least 72 h. (d) Section analysis of (c).

Herein, we also found that the size distribution of the nanospheres formed in THF was dependent on the concentration. As shown in Fig. 2, in the DLS plot, the average hydrodynamic diameter (D_h) of the spheres increases with the concentration of MCP-azo-OH. The average D_h varies from 137 nm to 265 nm as the concentration increases from 0.01 to 0.1 mg mL^{-1}. In this aspect, the self-assembly behaviour is different from that of the traditional amphiphilic molecules in that the size of the spherical micelles remains constant in a certain range of monomer concentration. The concentration-dependent size distribution feature is observed because the polymer molecules are associated by some supramolecular interactions in the spherical aggregates, which is proven by the following experiments.

As shown in Fig. 3a, in the ^1H NMR spectra, upon addition of a drop of D_2O, peaks at 10.3 and 7.9 ppm disappear and decrease in intensity, respectively. This phenomenon indicates that these two peaks represent two different active hydrogens, which went through proton exchange with deuterium of D_2O. The peak at 7.9 ppm is attributed to amide (H_b, Fig. 3a) on the main chain (deduced from gCOSY, gHSQC and gHMBC spectra, as shown in Fig. S4 in ESI†), and the peak around 10.3 ppm

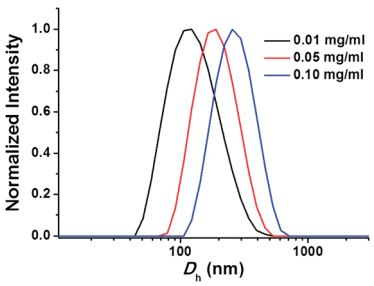

Fig. 2 D_h distributions of the nanospheres in THF with different concentration.

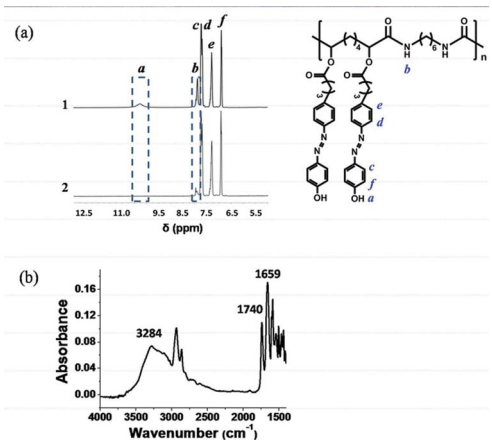

Fig. 3 (a) ^{1}H NMR spectra of MCP-azo-OH (a1) before and (a2) after addition of D_2O. (b) FTIR spectrum of MCP-azo-OH.

could represent the hydrogen (H_a, Fig. 3a) in the hydroxyl group. This result can also be confirmed by the FTIR spectrum (Fig. 3b), in which the vibration peaks of –OH and –NH– (the broad peak at around 3284 cm^{-1}) both shift to relatively lower wavenumbers compared to their isolated state (>3300 cm^{-1}). In addition, the peak at around 1659 cm^{-1} represents the vibrational absorption of carbonyl groups in amide, which normally stays at 1680 cm^{-1} without bonding. The bathochromic shift suggests that the carbonyl group should be involved in hydrogen bonds. At the same time, the vibrational absorption of carbonyl groups in ester bonds stays at around 1740 cm^{-1}, indicating that the carbonyl groups do not form any hydrogen bond. By summarising the above results, we can conclude that: (1) in the aggregates, the amide and hydroxyl groups are both involved in the formation of hydrogen bonds, but the ester groups are not; (2) due to the regularity of the molecular structure, associated intermolecular hydrogen bonds should exist between the molecules; and (3) the intermolecular hydrogen bonds should be responsible for the self-assembly of MCP-azo-OH in THF.

As described in the above discussion, the sizes of the nanospheres reflected by either the microscopic images or DLS have a very broad range. We were wondering if we could narrow the size distribution. Herein we found, by chance, a very interesting phenomenon. As we dropped the THF dispersion with nanospheres into water, a very small amount of precipitation appeared on the surface of the water. We carefully removed the precipitation and checked the nanospheres left in the water, and then we luckily obtained particles with a very narrow size distribution. Moreover, the average size could be adjusted by controlling the stirring rate of the water. Therefore, the relationship between the size distribution and stirring rate was also systematically studied, and the DLS results and corresponding AFM images are shown in Fig. 4. As a demonstration, the concentration of 0.5 mg mL^{-1} of MCP-azo-OH in THF was selected with a volume ratio of THF : water was 1 : 50. The average size of the nanospheres decreases with an increase in the stirring rate, as illustrated by the DLS data. Under the above mentioned conditions, the average D_h of the nanospheres is

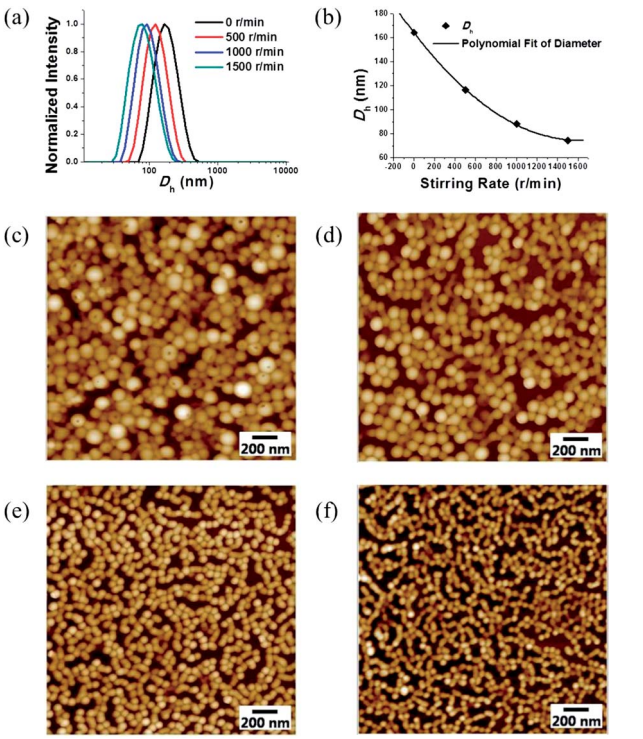

Fig. 4 (a) D_h of the nanospheres in aqueous suspensions prepared at different stirring rates measured by DLS. (b) Plot of the average D_h *versus* the stirring rate. The AFM images of the samples prepared at the stirring rates of (c) 0 rpm, (d) 500 rpm, (e) 1000 rpm, and (f) 1500 rpm. The method of preparing the suspensions is as follows: 100 μL THF suspension (0.5 mg mL^{-1}) of MCP-azo-OH was added into 5 mL water at a rate of one drop per minute at different stirring rates. After that, the suspensions were kept still for at least 24 h.

164 nm at the zero stirring rate, and when the stirring rate increases to 1500 rpm, the average D_h decreases to 74 nm. These data are consistent with those evaluated from the AFM images, as shown in Fig. 4c–f. When plotting the average D_h *versus* the stirring rate (Fig. 4b), it can be clearly seen that the average D_h tends to reach a plateau as the stirring rate is increased to 1500 rpm. Although the nanospheres formed in THF have a relatively large size distribution, the particles can be sorted according to size, and the size distribution (the data are listed in Tables S1 and S2 in the ESI†) is narrowed by dispersion in water with stirring. Very interestingly, after preparation in water, even if the stirring rate is further increased, the size of the nanospheres remains as it forms (ESI Fig. S5†). This result shows that the nanospheres are relatively stable when dispersed in water.

In the following experiment, the photo-responsive behavior of the nanospheres was investigated. Fig. 5a shows the UV-vis spectra upon irradiation by a 365 nm fiber lamp (about 40 mW cm^{-2}) equipped with a 30 mm diameter filter. The intensity of the peak at around 354 nm decreases with the irradiation time, indicating the *trans* to *cis* conformational conversion of the azobenzene group. The photo-responsive property is reflected not only in the conformational conversion of azobenzene, but also in the change in the size of the nanospheres. Taking the sample prepared by dropping THF suspension into water at

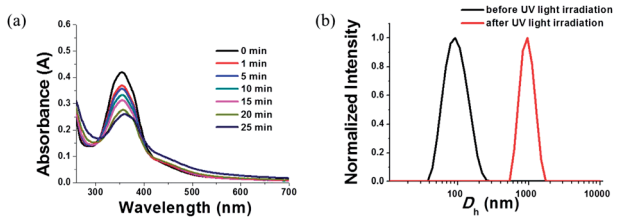

Fig. 5 (a) Variation of the UV-vis spectra of the aqueous suspension of MCP-azo-OH induced by UV light (365 nm) irradiation. (b) D_h distributions of the aggregates measured before and after UV light irradiation. The samples were prepared by dropping the THF suspension (0.5 mg mL^{-1}) into water at a stirring rate of 1000 rpm.

1000 rpm as an example, the average D_h increases from 88 nm to 1024 nm (DLS data in Fig. 5b) after irradiation for 25 min with 365 nm light. Since DLS uses a spherical model to fit the D_h of the particles, it cannot supply morphological information. Thus, in the following experiment, both AFM and TEM were utilized to investigate the microstructures of the aggregates before and after irradiation.

The aqueous suspension with a polymer concentration of 0.01 mg mL^{-1} was irradiated with 365 nm light for 25 min. The specimens before and after irradiation were observed by AFM and TEM. As shown in Fig. 6a and c, discrete nanospheres are obtained both in AFM and TEM images before irradiation. While after irradiation, the nanospheres seem to deform and aggregate into bigger clusters, showing a photo-induced deformation property. As mentioned above, the molecules in the aggregates have associated hydrogen bonds, which work as crosslinks between the molecules. Upon irradiation, we assume that the molecular level *trans* to *cis* conformational change of azobenzene groups will be magnified and induce the macroscopic deformation of the nanospheres. This deformation

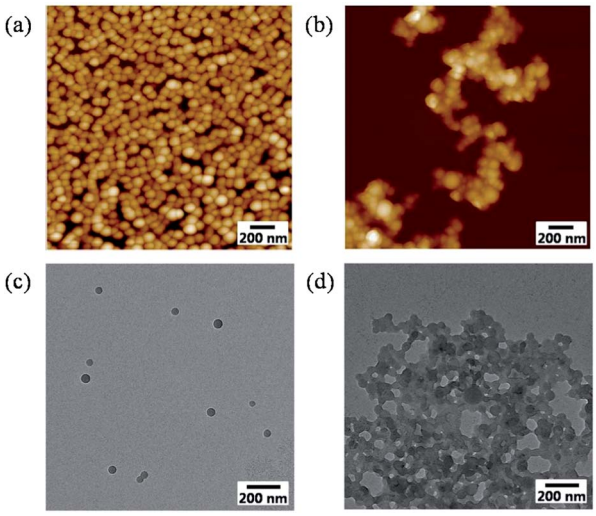

Fig. 6 AFM and TEM images of the nanospheres obtained from the aqueous suspension before and after UV light irradiation. (a) and (c) before UV light irradiation, (b) and (d) after 25 min of UV irradiation. The nanospheres were prepared by dropping the THF suspension (0.5 mg mL^{-1}) into water at the stirring rate of 1000 rpm.

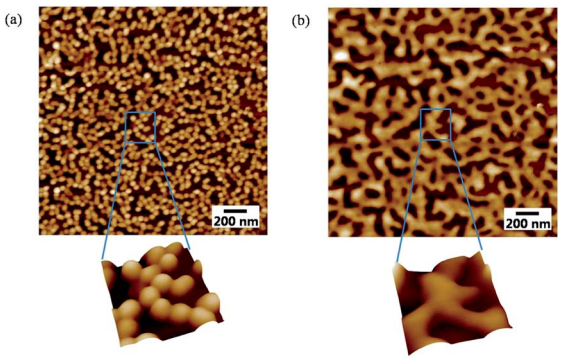

Fig. 7 AFM images of the nanospheres obtained from the aqueous suspension (a) before UV light irradiation and (b) after UV light irradiation for 15 min. The spheres were prepared by dropping the THF suspension (0.5 mg mL^{-1}) into water at the stirring rate of 1500 rpm.

should be responsible for the formation of the bigger clusters in water. Moreover, although the *trans* to *cis* conversion of the azobenzene group is reversible, the irradiation induced deformation is unfortunately not (refer to ESI Fig. S6†).

We were also wondering if the nanospheres still have the photo-induced property even in dry state. Thus, a sample was prepared referring to the conditions used to prepare the sample in Fig. 4f. UV light (365 nm) with a power of 20 mW cm^{-2} was used to *in situ* irradiate the sample for 15 min. As shown in Fig. 7, after irradiation, the nanospheres merged into island-like structures. The hydrogen bonds still exist after irradiation (ESI, Fig. S7†). During the irradiation, the hydrogen bonding should be responsible for the enlargement of the *trans* to *cis* conversion of the azobenzene groups, leading to the deformation of nanospheres. We were not sure if the deformation of nanospheres is induced by the possible heating effect due to the irradiation. Thus, we checked the temperature change during irradiation and found that such an irradiation power and dose barely caused an increase in temperature of the substrate. Moreover, a control of heating the sample to 40 °C and keeping that temperature for 1 h does not show any visible deformation of the nanospheres (ESI, Fig. S8†); therefore, the heating effect can be excluded.

IV Conclusions

We have synthesized an azobenzene-containing polymer MCP-azo-OH by MCP based on Passerini reaction and found that this molecule can self-assemble into spherical nanostructures. It has been proven that the associated intermolecular hydrogen bonds serve as supramolecular cross-links between the molecules. By dropping the THF suspension into water and controlling the stirring rate, the nanospheres can be sorted by their size. Either in aqueous medium or in dry state, the nanospheres can deform upon irradiation. We hope this type of research can provide a new clue for preparing nanostructured materials with photo-induced deformation properties.

Acknowledgements

The authors thank Professor Peter L. Rinaldi for his helpful discussion in the NMR interpretation. We would like to thank the National Natural Science Foundation of China (21204054) and the Project of Scientific and Technologic Infrastructure of Suzhou (SZS201207).

Notes and references

1 R. Lovrien, *Proc. Natl. Acad. Sci. U. S. A.*, 1967, **57**, 236.
2 H. Ringsdorf, B. Schlarb and J. Venzmer, *Angew. Chem., Int. Ed. Engl.*, 1988, **27**, 113.
3 T. Ikeda, S. Horiuchi, D. B. Karanjit, S. Kurihara and S. Tazuke, *Macromolecules*, 1990, **23**, 36.
4 T. Ikeda, S. Horiuchi, D. B. Karanjit, S. Kurihara and S. Tazuke, *Macromolecules*, 1990, **23**, 42.
5 T. Ikeda, S. Kurihara, D. B. Karanjit and S. Tazuke, *Macromolecules*, 1990, **23**, 3938.
6 M. Camacho-Lopez, H. Finkelmann, P. Palffy-Muhoray and M. Shelley, *Nat. Mater.*, 2004, **3**, 307.
7 T. Ikeda, J. I. Mamiya and Y. Yu, *Angew. Chem., Int. Ed.*, 2007, **46**, 506.
8 Y. Li, X. Tong, Y. He and X. Wang, *J. Am. Chem. Soc.*, 2006, **128**, 2220.
9 T. Kato, N. Mizoshita and K. Kishimoto, *Angew. Chem., Int. Ed.*, 2006, **45**, 38.
10 Y. Yu and T. Ikeda, *Macromol. Chem. Phys.*, 2005, **206**, 1705.
11 G. Shen, G. Xue, J. Cai, G. Zou, Y. Li and Q. Zhang, *Soft Matter*, 2013, **9**, 2512.
12 X. Liu and M. Jiang, *Angew. Chem., Int. Ed.*, 2006, **45**, 3846.
13 Y. Yu and T. Ikeda, *Angew. Chem., Int. Ed.*, 2006, **45**, 5416.
14 Y. Yu, T. Maeda, J. I. Mamiya and T. Ikeda, *Angew. Chem., Int. Ed.*, 2007, **46**, 881.
15 M. Yamada, M. Kondo, J. I. Mamiya, Y. Yu, M. Kinoshita, C. J. Barrett and T. Ikeda, *Angew. Chem., Int. Ed.*, 2008, **47**, 4986.
16 Y. Zhao and T. Ikeda, *Smart Light-Responsive Materials: Azobenzene-Containing Polymers and Liquid Crystals*, John Wiley & Sons, 2008.
17 J. Wei, Y. Liu, J. Chen, Y. Li, Q. Yue, G. Pan, Y. Yu, Y. Deng and D. Zhao, *Adv. Mater.*, 2013, **26**, 1782.
18 S. Lee, S. Oh, J. Lee, Y. Malpani, Y. S. Jung, B. Kang, J. Y. Lee, K. Ozasa, T. Isoshima, S. Y. Lee, M. Hara, D. Hashizume and J. M. Kim, *Langmuir*, 2013, **29**, 5869.
19 J. del Barrio, E. Blasco, L. Oriol, R. Alcala and C. Sanchez-Somolinos, *J. Polym. Sci., Part A: Polym. Chem.*, 2013, **51**, 1716.
20 K. Chen, G. Xue, G. Shen, J. Cai, G. Zou, Y. Li and Q. Zhang, *RSC Adv.*, 2013, **3**, 8208.
21 Y. Wang, S. Lin, M. Zang, Y. Xing, X. He, J. Lin and T. Chen, *Soft Matter*, 2012, **8**, 3131.
22 G. Shen, G. Xue, J. Cai, G. Zou, Y. Li, M. Zhong and Q. Zhang, *Soft Matter*, 2012, **8**, 9127.
23 A. Priimagi, A. Shimamura, M. Kondo, T. Hiraoka, S. Kubo, J. I. Mamiya, M. Kinoshita, T. Ikeda and A. Shishido, *ACS Macro Lett.*, 2012, **1**, 96.
24 K. M. Lee, D. H. Wang, H. Koerner, R. A. Vaia, L. S. Tan and T. J. White, *Angew. Chem., Int. Ed.*, 2012, **51**, 4117.
25 S. Wu, L. Wang, A. Kroeger, Y. Wu, Q. Zhang and C. Bubeck, *Soft Matter*, 2011, **7**, 11535.
26 J. Vapaavuori, V. Valtavirta, T. Alasaarela, J. I. Mamiya, A. Priimagi, A. Shishido and M. Kaivola, *J. Mater. Chem.*, 2011, **21**, 15437.
27 O. Boissiere, D. Han, L. Tremblay and Y. Zhao, *Soft Matter*, 2011, **7**, 9410.
28 T. Ikeda and O. Tsutsumi, *Science*, 1995, **268**, 1873.
29 A. Buguin, M. H. Li, P. Silberzan, B. Ladoux and P. Keller, *J. Am. Chem. Soc.*, 2006, **128**, 1088.
30 M. Alonso, V. Reboto, L. Guiscardo, A. San Martin and J. C. 0020Rodriguez-Cabello, *Macromolecules*, 2000, **33**, 9480.
31 A. Athanassiou, M. Kalyva, K. Lakiotaki, S. Georgiou and C. Fotakis, *Adv. Mater.*, 2005, **17**, 988.
32 A. Mamada, T. Tanaka, D. Kungwatchakun and M. Irie, *Macromolecules*, 1990, **23**, 1517.
33 J. Gao, Y. He, F. Liu, X. Zhang, Z. Wang and X. Wang, *Chem. Mater.*, 2007, **19**, 3877.
34 J. Gao, Y. He, H. Xu, B. Song, X. Zhang, Z. Wang and X. Wang, *Chem. Mater.*, 2007, **19**, 14.
35 A. Natansohn and P. Rochon, *Chem. Rev.*, 2002, **102**, 4139.
36 E. Ishow, B. Lebon, Y. N. He, X. G. Wang, L. Bouteiller, L. Galmiche and K. Nakatani, *Chem. Mater.*, 2006, **18**, 1261.
37 O. M. Tanchak and C. J. Barrett, *Macromolecules*, 2005, **38**, 10566.
38 K. G. Yager, O. M. Tanchak, C. Godbout, H. Fritzsche and C. J. Barrett, *Macromolecules*, 2006, **39**, 9311.
39 C. J. Barrett, J. I. Mamiya, K. G. Yager and T. Ikeda, *Soft Matter*, 2007, **3**, 1249.
40 M. C. Jimenez, C. Dietrich-Buchecker and J. P. Sauvage, *Angew. Chem., Int. Ed.*, 2000, **39**, 3284.
41 S. Courty, J. Mine, A. R. Tajbakhsh and E. M. Terentjev, *Europhys. Lett.*, 2003, **64**, 654.
42 C. L. van Oosten, C. W. M. Bastiaansen and D. J. Broer, *Nat. Mater.*, 2009, **8**, 677.
43 C. J. Camargo, H. Campanella, J. E. Marshall, N. Torras, K. Zinoviev, E. M. Terentjev and J. Esteve, *J. Micromech. Microeng.*, 2012, **22**, 075009.
44 Q. Qian, J. Chen, M. H. Li, P. Keller and D. He, *J. Mater. Chem.*, 2012, **22**, 4669.
45 T. J. White, N. V. Tabiryan, S. V. Serak, U. A. Hrozhyk, V. P. Tondiglia, H. Koerner, R. A. Vaia and T. J. Bunning, *Soft Matter*, 2008, **4**, 1796.
46 S. Serak, N. Tabiryan, R. Vergara, T. J. White, R. A. Vaia and T. J. Bunning, *Soft Matter*, 2010, **6**, 779.
47 Y. Li, Y. He, X. Tong and X. Wang, *J. Am. Chem. Soc.*, 2005, **127**, 2402.
48 J. Liu, Y. He and X. Wang, *Polymer*, 2010, **51**, 2879.
49 Y. Wang, P. Han, H. Xu, Z. Wang, X. Zhang and A. V. Kabanov, *Langmuir*, 2010, **26**, 709.
50 N. Ma, Y. Wang, B. Wang, Z. Wang, X. Zhang, G. Wang and Y. Zhao, *Langmuir*, 2007, **23**, 2874.
51 Q. Jin, G. Liu, X. Liu and J. Ji, *Soft Matter*, 2010, **6**, 5589.
52 Y. Wang, N. Ma, Z. Wang and X. Zhang, *Angew. Chem., Int. Ed.*, 2007, **46**, 2823.

53 S. Wu, S. Duan, Z. Lei, W. Su, Z. Zhang, K. Wang and Q. Zhang, *J. Mater. Chem.*, 2010, **20**, 5202.
54 Z. Feng, L. Lin, Z. Yan and Y. Yu, *Macromol. Rapid Commun.*, 2010, **31**, 640.
55 Q. Yuan, Y. Zhang, T. Chen, D. Lu, Z. Zhao, X. Zhang, Z. Li, C. H. Yan and W. Tan, *ACS Nano*, 2012, **6**, 6337.
56 E. Blasco, J. del Barrio, C. Sanchez-Somolinos, M. Pinol and L. Oriol, *Polym. Chem.*, 2013, **4**, 2246.
57 J. M. Schumers, C. A. Fustin and J. F. Gohy, *Macromol. Rapid Commun.*, 2010, **31**, 1588.
58 B. Yan, X. Tong, P. Ayotte and Y. Zhao, *Soft Matter*, 2011, **7**, 10001.
59 E. Blasco, J. Luis Serrano, M. Pinol and L. Oriol, *Macromolecules*, 2013, **46**, 5951.
60 J. F. Gohy and Y. Zhao, *Chem. Soc. Rev.*, 2013, **42**, 7117.
61 O. Kreye, T. Toth and M. A. R. Meier, *J. Am. Chem. Soc.*, 2011, **133**, 1790.
62 X. X. Deng, L. Li, Z. L. Li, A. Lv, F. S. Du and Z. C. Li, *ACS Macro Lett.*, 2012, **1**, 1300.
63 Y. Z. Wang, X. X. Deng, L. Li, Z. L. Li, F. S. Du and Z. C. Li, *Polym. Chem.*, 2013, **4**, 444.
64 R. Kakuchi, *Angew. Chem., Int. Ed.*, 2014, **53**, 46.
65 C. Zhu, B. Yang, Y. Zhao, C. Fu, L. Tao and Y. Wei, *Polym. Chem.*, 2013, **4**, 5395.
66 Y. Zhao, B. Yang, C. Zhu, Y. Zhang, S. Wang, C. Fu, Y. Wei and L. Tao, *Polym. Chem.*, 2014, **5**, 2695.
67 Y. Zhang, Y. Zhao, B. Yang, C. Zhu, Y. Wei and L. Tao, *Polym. Chem.*, 2014, **5**, 1857.